

Effective kinematic viscosity of turbulent He II

T. V. Chagovets,¹ A. V. Gordeev,¹ and L. Skrbek²

¹*Institute of Physics ASCR, v.v.i., Na Slovance 2, 182 21 Prague, Czech Republic*

²*Faculty of Mathematics and Physics, Charles University, V Holešovičkách 2, 180 00 Prague, Czech Republic*

(Received 26 March 2007; published 7 August 2007)

The temperature dependence of the effective kinematic viscosity of turbulent He II, $\nu_{eff}(T)$, is deduced from second sound attenuation data using the late stage of decay of thermally induced counterflow He II turbulence in two channels of square cross section. It is shown to qualitatively agree with the published data for $\nu_{eff}(T)$ calculated based on experiments on decaying-grid-generated He II turbulence [Niemela *et al.*, *J. Low Temp. Phys.* **138**, 537 (2005)]. Corrections to these data due to the “sine squared” law that describes attenuation of the second sound wave propagating along an arbitrary direction with respect to the direction of the core of a quantized vortex in turbulent He II are discussed and applied.

DOI: [10.1103/PhysRevE.76.027301](https://doi.org/10.1103/PhysRevE.76.027301)

PACS number(s): 47.27.Gs, 47.37.+q, 67.40.Vs

Quantum turbulence in He II has been the subject of numerous experimental and theoretical investigations (see the reviews [1,2] and references therein) since the experiments of Vinen [3] half a century ago. The early experiments were almost entirely devoted to counterflow turbulence, which is easy to generate by applying heat to the dead end of the flow channel. Many aspects of steady-state counterflow He II turbulence can be understood in the frame of the phenomenological theory of Vinen [3], later backed by the numerical simulations of Schwarz [4].

During the last 15 years, interest shifted toward He II turbulence generated classically, e.g., between counterrotating disks [5] or by towing a grid of bars through a stationary sample of He II [6–9]. These experiments show that classically generated He II turbulence is very similar in its characteristics to classical turbulence in viscous fluids, despite the two-fluid behavior of He II and quantization of circulation in its superfluid component. The experiments of Maurer and Tabeling [5] strongly suggest the existence of the a three-dimensional (3D) energy spectrum in He II turbulence containing an inertial range of scales of the classical form $C\varepsilon^{2/3}k^{-5/3}$ [10], where k denotes the wave number and $\varepsilon = -dE/dt$ is the energy decay rate. Moreover, from measurements of the skewness factor of the velocity increments, these authors found the value of the 3D Kolmogorov constant $C \cong 1.5$, which corresponds to the accepted value in classical turbulence [11]. The experimentally observed decay of the vortex line density L (the total length of the vortex line in a unit volume of He II) in grid-generated He II turbulence has been found essentially classical [6–9] in that it can be closely described by a purely classical decay model for vorticity $\boldsymbol{\omega} = \text{curl } \mathbf{v}$, if the rms superfluid vorticity is defined as $\omega = \kappa L$, where κ denotes the quantum of circulation [12]. Vinen [13] argued that at large length scales the normal fluid and the superfluid are coupled and behave as a single-component conventional fluid, and that the rate of dissipation of turbulent flow energy is likely to be given by an expression similar to that in a conventional fluid with a temperature-dependent effective kinematic viscosity:

$$\varepsilon = \nu_{eff}\omega^2 = \nu_{eff}(T)\kappa^2L^2. \quad (1)$$

In view of the link between He II turbulence and classical turbulence, having in mind the possibility of practical use of He II as a working fluid [14,15], it is important to know the effective kinematic viscosity and its temperature dependence. One way of determining it is to use the second sound data on decaying vortex line density in grid-generated He II turbulence (such as are published in Refs. [16,7]), as was first done by Stalp and co-workers in [17]. This method is based on the classical decay model [7,8,12] for vorticity defined as κL , namely, on the third universal regime of its decay occurring after saturation of the energy-containing length scale by the size of the channel, D . Experimentally, typically two to three orders of magnitude of the decaying L closely obey the power law

$$L(t) = \frac{D(3C)^{3/2}}{2\pi\kappa\sqrt{\nu_{eff}}}(t + t_{vo})^{-3/2} \cong \frac{D(3C)^{3/2}}{2\pi\kappa\sqrt{\nu_{eff}}}t^{-3/2}, \quad (2)$$

where C is the 3D Kolmogorov constant and t_{vo} stands for the virtual origin time, which for most of the decay typically satisfies the condition $t \gg t_{vo}$ and can be neglected. By comparing the experimental decay data of L measured at various temperatures with Eq. (2), values of $\nu_{eff}(T)$ can be easily extracted. Let us stress that extracting the kinematic viscosity from the data for classical decaying turbulence is not possible—kinematic viscosity does not enter the energy decay law and vorticity cannot be measured in experiments with viscous working fluids.

As for the thermally generated counterflow turbulence in He II, it was commonly assumed that it had nothing in common with classical turbulence. While there might indeed be little in common between developed classical turbulence and steady-state counterflow turbulence, which is well described by the phenomenological Vinen equation [2,3], the temporal decay of counterflow turbulence certainly does not obey the simple consequence of this equation: at late time $L(t)$ is predicted to decay inversely proportionally to time. On the contrary, experimental data on decaying counterflow turbulence display a very complex decay process. For a full picture of the underlying physics we direct the reader to a recent review

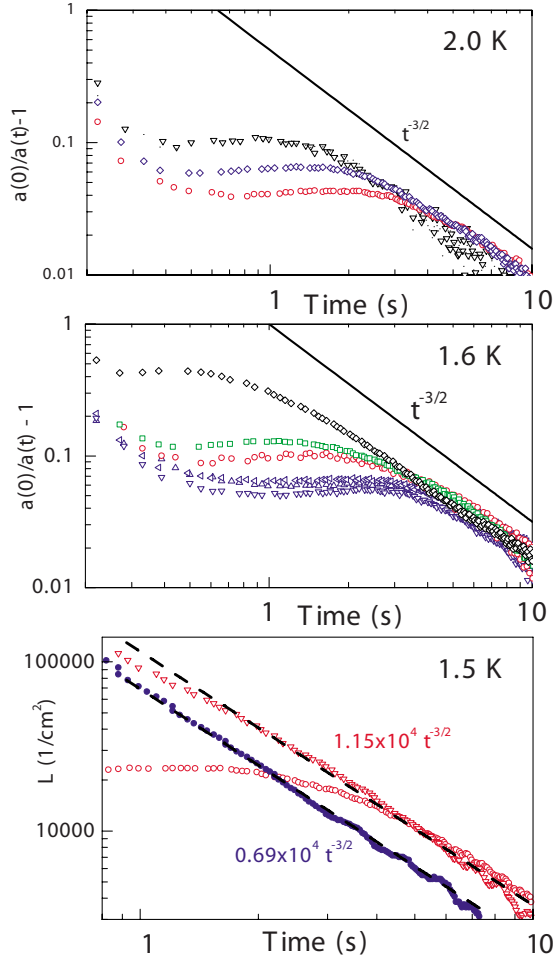


FIG. 1. (Color online) Examples of the second sound experimental data. The top and middle figures show logarithmic plots of the quantity $a(0)/a(t)-1$ versus time, measured in the $1 \times 1 \text{ cm}^2$ channel. Under the assumption that the tangle is homogeneous and isotropic, this quantity would be proportional to L , via Eq. (3). The decay curves measured at $T=2 \text{ K}$ originate from the steady-state counterflow generated by applying 0.52 W (∇), 0.41 W (\diamond , blue online), and 0.32 W (\circ , red online); the decay curves at $T=1.6 \text{ K}$ from 0.5 W (\diamond), 0.23 W (squares, green online), 0.18 W (\circ , red online), and 0.14 W (various triangles, blue online; three individual decay curves are shown to show the level of reproducibility for the lowest applied power). The bottom figure shows the decaying L calculated using formula (3) from the second sound data measured in both channels assuming that the decaying turbulence is homogeneous and isotropic. The third universal decay regime (the power law decay with the exponent of $-3/2$ represented by dashed lines) is reached irrespectively of the initial conditions, as once more demonstrated by the two decay curves measured in the $1 \times 1 \text{ cm}^2$ channel (open symbols, red online). The decay data measured in the $0.6 \times 0.6 \text{ cm}^2$ channel (filled symbols, blue online) also follow the third universal decay regime but with the prefactor lowered by 0.6, the ratio of the channels widths, in accord with Eq. (2).

[18], where current understanding of decaying counterflow He II turbulence is described in detail.

Examples of the measured decay curves are shown in Fig. 1. We show the quantity $a(0)/a(t)-1$, where $a(t)$ is the recovering amplitude of the transverse second sound standing

mode and $a(0)$ is the unperturbed amplitude with no applied heat in the channel. Note that the relative amplitude requires no calibration. The second sound standing wave across the channel is generated and detected by the gold-plated Nuclepore transmitter and receiver mounted in the opposing walls of the channel in the middle of its length [16,18,19]. The absorption and dispersion signal is detected by the two-phase lock-in amplifier. Scanning the driving frequency across one of the resonant peaks (typically the second one, occurring around 2 kHz) with no heat applied to the channel and fitting to a Lorentzian gives the linewidth Δ_0 . The system is then tuned to resonance. The heater in the channel is switched on for typically 10 s (resulting in the generation of steady-state counterflow turbulence) and off again, while $a(t)$ is recorded during the decay.

It is known that the vortex tangle generated by steady-state counterflow is polarized. Without knowing the degree of polarization, the second sound amplitude alone does not provide enough information to calculate the total vortex line density. This is why we plot the quantity $a(0)/a(t)-1$ in the upper part of Fig. 1, rather than the total vortex line density, which we do not know. On the other hand, it has been shown that the degree of polarization decreases during the decay [18,20] and causes the almost flat middle part of the decay. Here we are concerned with the late stage of the decay—precisely with the *third universal decay regime*, over which the vortex tangle could be assumed homogeneous and isotropic. Our previously published data [18,21,22] as well as examples given in Fig. 1 clearly display up to two orders of magnitude of the classical $t^{-3/2}$ power law decay. This form of the decay is independent of temperature over the range that we investigated. Thus for late times the decay of counterflow turbulence and the decay of grid-generated turbulence are essentially similar. As demonstrated in the bottom picture of Fig. 1, this similarity is further strengthened by the fact that the late decay follows the pattern predicted by the phenomenological spectral decay model for decaying vorticity in the form of Eq. (2) in that the observed decaying vortex line density (or mean superfluid vorticity defined as $\langle \omega \rangle = \kappa L$) is proportional to the channel size [18,21].

Hence our experimental decay data obtained for two channels allow deducing the temperature dependence of the effective kinematic viscosity from the late decay of counterflow He II turbulence, essentially in the same way as has been done for the grid-generated turbulence decay data [9,17]. For these calculations, we have used $C=1.5$ [5,11] and tabulated values of He II properties [23]. We assume that over the relevant time range the decaying vortex tangle is homogeneous and isotropic [18]. The results of our analysis for both channels of square cross section are displayed in Fig. 2.

While evaluating $\nu_{eff}(T)$, we have avoided a small systematic error that is present in published calculations of this quantity from the grid-generated turbulence decay data [9,15,17]. The reason for it is as follows. What is detected by the second sound sensors is neither the total length of the quantized vortex line in the resonator, nor the individual projected lengths. It can be shown [20] that the attenuation of a second sound wave of angular frequency ω in the presence

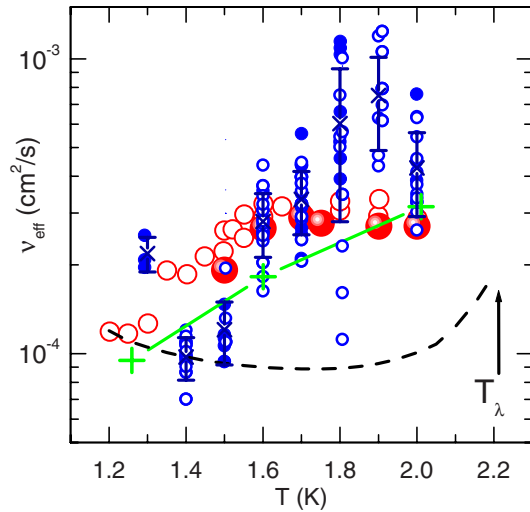


FIG. 2. (Color online) Temperature dependence of the effective kinematic viscosity of turbulent He II. The small open circles (blue online) are the data deduced from the late stage of decaying counterflow turbulence in the square channel of cross section $1 \times 1 \text{ cm}^2$; the small filled circles (blue online) from the smaller channel $0.6 \times 0.6 \text{ cm}^2$. The crosses with error bars (navy-blue online) represent the mean value over our data from both channels at each temperature. Big circles (red online) are corrected data (see text) from Fig. 2 of [9], deduced from the decaying vortex line density in the experiments of Donnelly and co-workers with unconventional (open big circles) and conventional (filled big circles) grids. The crosses connected by the solid line (green online) represent a model calculation for $\nu_{eff}(T)$ [2]. The dashed line is a plot of kinematic viscosity of He II based on the total fluid density [23].

of a straight vortex line is $\sin^2(\theta)\omega B/(2\Omega)$, where θ is the angle between the direction of the quantized vorticity and the direction of second sound propagation. This “sine squared” law has been confirmed by measuring second sound signals in a container of helium held at tilted angles with respect to the axis of rotation of the cryostat [24]. If the tangle is assumed isotropic, since $\langle \sin^2(\gamma) \rangle = 2/3$, where $\langle \rangle$ denotes the average over the unit sphere, the second sound sensors detect $L_{eff} = 2L/3$, where L is the actual vortex line density. Applying this to the case of a homogeneous vortex tangle [18,20] and taking into account that vortices oriented parallel to the second sound propagation do not contribute to the excess attenuation, we have

$$L = \frac{6\pi\Delta_0}{B\kappa} \left(\frac{a_0}{a} - 1 \right) \quad (3)$$

as opposed to

$$L = \frac{16\Delta_0}{B\kappa} \left(\frac{a_0}{a} - 1 \right), \quad (4)$$

where the prefactor $\pi/4$ was applied, based on the geometrical projection of a random vortex tangle to the plane perpendicular to the second sound wave. Let $p = a_0/a$ and $P = 1 - \cos(2\pi d\Delta_0/u_2)$, then, for $d\Delta_0/u_2 \ll 1$, it can be shown that a more precise formula is [20]

$$L = \frac{3u_2}{B\kappa d} \ln \left(\frac{1 + p^2P + \sqrt{2p^2P + p^4P^2}}{1 + P + \sqrt{2P + P^2}} \right), \quad (5)$$

as opposed to

$$L = \frac{8u_2}{\pi B\kappa d} \ln \left(\frac{1 + p^2P + \sqrt{2p^2P + p^4P^2}}{1 + P + \sqrt{2P + P^2}} \right), \quad (6)$$

first derived in Ref. [16], where the sine squared law was not taken into account. All values of L reported in the experiments of Donnelly and co-workers [6–8,16,17] and of Skrbek and co-workers [21,22] experiments must thus be multiplied by a factor of $3\pi/8 \approx 1.2$. This is only a minor correction as far as decaying turbulence is concerned, but affects the effective kinematic viscosity as published in Refs. [9,17] derived from the grid turbulence decay data, which is $(3\pi/8)^2 \approx 1.4$ too low.

Let us compare our data deduced from the decaying He II counterflow turbulence with the *corrected* effective kinematic viscosity data obtained from the towed grid experiment [9,17] also shown in Fig. 2. Such a comparison is justified and useful, as in the experiments we have used the same square $1 \times 1 \text{ cm}^2$ channel (plus a smaller one $0.6 \times 0.6 \text{ cm}^2$) and essentially the same second sound technique [18,19,21,22].

The original second sound data on decaying He II turbulence [6–8,16,17] were obtained using a grid of a rather unconventional design in that the 65% open grid consisted of only four parallel rectangular tines crossed by a single tine at 45° , to which a centered pull rod was attached. This might have caused a difference in the nature of turbulence generated by such a grid with respect to turbulence generated by a grid of conventionally accepted geometry. Therefore Niemela and co-workers [9] later repeated measurements of decaying vortex line density in the same $1 \times 1 \text{ cm}^2$ channel using a newly designed grid consisting of 28 rectangular tines of width 0.012 cm forming 13×13 full meshes across a channel of approximate dimension $M = 0.064 \text{ cm}$. That the decay data indeed follow the $-3/2$ power law very closely is further strengthened by an additional analysis (see Fig. 9 in Ref. [15]). Values of $\nu_{eff}(T)$ deduced from the decay data originating from relatively high-mesh Reynolds number turbulence $\text{Re}_M = v_g M \rho / \mu$ of order 10^5 , where v_g is the grid velocity, M is the mesh size, ρ is the total density of He II, and μ its dynamic viscosity, do not differ dramatically from the data obtained with the original unconventional grid, although they systematically lie about 10% lower (see Fig. 2).

The towed-grid- and counterflow-generated data series are consistent with each other, the counterflow data displaying larger scatter. The displayed error bars reflect only the statistical scatter of the data, which is mostly caused by the fact that for generating counterflow turbulence a large heat input up to 1 W has to be applied to the dead end of the channel and then abruptly switched off. Although in the experiment the total heat input to the cryostat is kept constant (the power is not switched off but to another matching heater placed outside the channel in the helium bath), it is very difficult to stabilize the bath temperature, even with an additional bath heater and a temperature controller in use. Minimizing the

temperature fluctuations that necessarily follow switching off the channel heater is an experimental challenge. Fine tuning of the electronics at any particular temperature is needed before reproducible decay curves closely following the $-3/2$ power law (such as shown in Fig. 1 and in [18,21,22]) can be measured. This becomes increasingly difficult at both the lowest and highest displayed temperatures and hardly possible above 2 K, where the second sound velocity steeply depends on temperature, and therefore temperature fluctuations affect the propagation of second sound in the channel more strongly. Another source of a systematic error might be coupling between transverse and longitudinal second sound modes in the channel, which could lead to slightly distorted values of the linewidth Δ_0 entering Eq. (3).

Within experimental error, the calculated values of $\nu_{eff}(T)$ for two square channels do not depend on the channel size, in accord with Eq. (2). It is clear that the effective kinematic viscosity of *turbulent* He II $\nu_{eff}(T)$ distinctly differs from the tabulated values of kinematic viscosity of He II [23] defined as the dynamic viscosity over the total density, $\nu = \mu/\rho$ (see the dotted line in Fig. 2). A model calculation [2] based on

the assumption that the effective kinematic viscosity is entirely due to mutual friction is also included in Fig. 2.

In conclusion, we present experimental values of the effective kinematic viscosity of turbulent He II, over the temperature range where the temporal decays of thermal counterflow and towed-grid turbulence have been investigated using the second sound attenuation technique. It is remarkable that, although the steady states of the grid-generated turbulence in He II and the thermally induced counterflow He II turbulence are very different in character [2], their late decays display a universal classical power law of the form of Eq. (2); moreover, the deduced values of effective kinematic viscosity are consistent with each other as well as with the model calculation [2].

The authors appreciate stimulating discussions with J. J. Niemela, K. R. Sreenivasan, and W. F. Vinen. This research is supported by Research Contracts No. MS 0021620834 and No. AVOZ 10100520 and by GAČR under Grant No. 202/05/0218.

-
- [1] J. T. Tough, *Superfluid Turbulence*, in Progress in Low Temperature Physics, Vol. 8 (North-Holland, Amsterdam, 1982).
- [2] W. F. Vinen and J. J. Niemela, J. Low Temp. Phys. **128**, 167 (2002).
- [3] H. E. Hall and W. F. Vinen, Proc. R. Soc. London, Ser. A **238**, 204, 205 (1956); W. F. Vinen, *ibid.* **240**, 114 (1957); **240**, 128 (1957); **242**, 489 (1957).
- [4] K. W. Schwarz, Phys. Rev. B **38**, 2398 (1988).
- [5] J. Maurer and P. Tabeling, Europhys. Lett. **43**, 29 (1998).
- [6] M. R. Smith, R. J. Donnelly, N. Goldenfeld, and W. F. Vinen, Phys. Rev. Lett. **71**, 2583 (1993).
- [7] S. R. Stalp, L. Skrbek, and R. J. Donnelly, Phys. Rev. Lett. **82**, 4831 (1999).
- [8] L. Skrbek, J. J. Niemela, and R. J. Donnelly, Phys. Rev. Lett. **85**, 2973 (2000).
- [9] J. J. Niemela, K. R. Sreenivasan, and R. J. Donnelly, J. Low Temp. Phys. **138**, 537 (2005).
- [10] It was also shown that intermittency survives below T_λ ; moreover, the deviation from Kolmogorov exponents are indistinguishable from those in classical turbulence.
- [11] K. R. Sreenivasan, Phys. Fluids **7**, 2778 (1995).
- [12] L. Skrbek and S. R. Stalp, Phys. Fluids **12**, 1997 (2000).
- [13] W. F. Vinen, Phys. Rev. B **61**, 1410 (2000).
- [14] L. Skrbek, J. J. Niemela, and R. J. Donnelly, J. Phys.: Condens. Matter **11**, 7761 (1999).
- [15] J. J. Niemela and K. R. Sreenivasan, J. Low Temp. Phys. **143**, 163 (2006).
- [16] S. R. Stalp, Ph.D. thesis, University of Oregon, Eugene, 2000.
- [17] S. R. Stalp, J. J. Niemela, W. F. Vinen, and R. J. Donnelly, Phys. Fluids **14**, 1377 (2002).
- [18] C. F. Barenghi and L. Skrbek, J. Low Temp. Phys. **146**, 5 (2007).
- [19] T. V. Chagovets *et al.*, Acta Phys. Slov. **56**, 169 (2006).
- [20] C. F. Barenghi, A. V. Gordeev, and L. Skrbek, Phys. Rev. E **74**, 026309 (2006).
- [21] A. V. Gordeev, T. V. Chagovets, F. Soukup, and L. Skrbek, J. Low Temp. Phys. **138**, 549 (2005).
- [22] L. Skrbek, A. V. Gordeev, and F. Soukup, Phys. Rev. E **67**, 047302 (2003).
- [23] R. J. Donnelly and C. F. Barenghi, J. Phys. Chem. Ref. Data **27**, 1217 (1998).
- [24] H. A. Snyder and Z. Putney, Phys. Rev. **150**, 110 (1966); P. Mathieu, B. Placais, and Y. Simon, Phys. Rev. B **29**, 2489 (1984).